1st International Conference on Sensing Technology
November 21-23, 2005 Palmerston North, New Zealand

Global Calibration Based on Local Calibration for an Ultrasonic Location Sensor*

Akifumi Nishitani
Tokyo University of Science
2641, Yamazaki, Noda-shi, Chiba, 278-8510, Japan
a-nishitani@aist.go.jp

Yoshifumi Nishida
Digital Human Research Center, AIST & CREST, JST
2-41-6, Aomi, Koto-ku, Tokyo, 135-0064, Japan
y.nishida@aist.go.jp

Toshio Hori
Digital Human Research Center, AIST & CREST, JST
2-41-6, Aomi, Koto-ku, Tokyo, 135-0064, Japan
t.hori@aist.go.jp

Takeo Kanade
Digital Human Research Center, AIST & CREST, JST
2-41-6, Aomi, Koto-ku, Tokyo, 135-0064, Japan
t.kanade@aist.go.jp

Hiroshi Mizoguchi
Tokyo University of Science
2641, Yamazaki, Noda-shi, Chiba, 278-8510, Japan
hm@rs.noda.tus.ac.jp

***Abstract*— The ability to quickly construct a human activity observation system is required in order to conduct field research on human activities. The authors have developed an ultrasonic location system, which is a type of location sensing system for observing human activities. The present study attempts to establish a systematic method for quickly constructing an ultrasonic location system in various environments. A calibration function that can be used in various environments is one of the basic functions of the ultrasonic location system. In the present paper, we propose a new calibration method, "global calibration based on local calibration (GCLC)," for calibrating the 3D positions of ultrasonic receivers placed arbitrarily in a daily-use environment. The proposed method requires a relatively small number of transmitters and is independent of room size. In addition, we describe two constraints that can be used in conjunction with the GCLC method. The performance of the GCLC method was investigated in an experimental room (4.0×4.0×2.7 m), in which 80 ultrasonic receivers were attached to the ceiling. A portable system based partly on the proposed method is also presented herein.**

***Keywords*— human activity obervation, ultrasonic location sensor, calibration.**

I. Introduction

Recently, human-centered information processing services have been attracting increasing attention. The goal of the present research is to establish a technique by which to recognize both human activity and the state in a living space. Therefore, it is necessary to observe human activity in real time and with high accuracy, without the presence of constraints that prevent natural human activities.

As a method for efficient and robust recognition of activities in a daily environment, the concept of object-based activity recognition has been proposed. The behavior of handling objects in an environment such as an office or home can be recognized based on the motion of the objects [1]. We have developed a three-dimensional (3D) ultrasonic location system as a fundamental system for robustly tracking objects and have verified that the observation of human activity based on object tracking is possible [2], [3]. However, like other location sensors, the developed ultrasonic location sensor has a disadvantage in that lack of portability makes it difficult to collect activity data in the various environments in which actual human activities occur.

In the present paper, we propose a rapid calibration method, "global calibration based on local calibration," that enables users to quickly calibrate the positions of ultrasonic receivers of an ultrasonic location system and observe the system for field research on human activities.

II. Related Work

Several types of ultrasonic location systems have been proposed. The Bat Ultrasonic Location System [4–7] developed by AT&T, and the MIT Cricket Indoor Location System [8] are well known. Although a calibration method using a robot [9] has been proposed, the required calibration device is too large for use in a number of environments. An auto calibration method was considered in the DOLPHIN system [10], which can calibrate the positions of receivers/transmitters using a small number of reference receivers/transmitters having known positions. However, the system has only been tested in narrow areas having dimensions of approximately 2.5 m × 2 m. Bristol University proposed another auto calibration method, in which the positions of n transmitters and m receivers can be calculated given n×m distance data among the transmitters and receivers and that the condition, $3(n+m)-6 < n\cdot m$, is satisfied [11]. However, the scalability of this method is limited.

In contrast, the present study proposes and examines a new calibration method, "global calibration based on local calibration," that requires a relatively small number of transmitters and is independent of room size. Using the proposed method, the calibration problem becomes a similar to a fitting problem in object modeling with multiple range images [12], [13] after local calibration. The

*This study was supported in part by a Grant-in-Aid as part of the Special Coordination Fund for Promoting Science and Technology from the Ministry of Education, Culture, Sports, Science and Technology of Japan.

present paper describes the method for global calibration based on local calibration and the constraints that are used in conjunction with the method for reducing the error of the calibrated receiver positions.

III. Quick Calibration Method

A. Proposal of a rapid calibration method

In the present paper, in addition to the "global calibration based on local calibration (GCLC)" method, we propose two constraints that can be used in conjunction with the GCLC method, as described below.

The procedure for GCLC is described below.

1. Move the calibration device arbitrarily to multiple positions (A, B, and C in Fig. 1).
2. Calculate the positions of the receivers in a local coordinate system, with the local origin set at the position of the calibration system.
3. Select receivers for which the positions can be calculated from more than two calibration system positions.
4. Select a global coordinate system from among the local coordinate systems and calculate the positions of the calibration device in the global coordinate system using the receivers selected in Step 3. Then, calculate transformation matrices (M_1 and M_2 in Fig. 1).
5. Calculate the receiver positions using the receiver positions calculated in Step 2 and the transformation matrices calculated in Step 4.

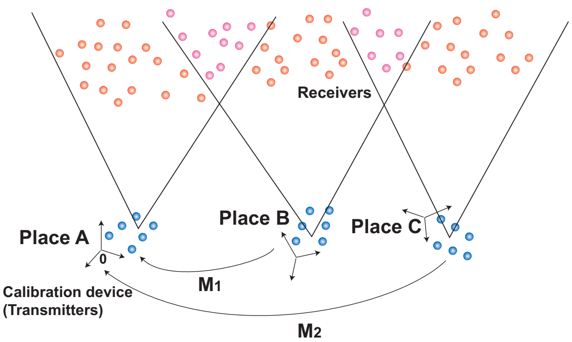

Fig. 1. Quick calibration method 1

Steps 2 and 4 are described in detail in the following.

B. Linear method for rapid calibration

1) Calculating the 3D positions of receivers in a local coordinate system based on distance data (Step 2): The receiver position (x,y,z) is calculated by a multilateration algorithm, such as that used in the Global Positioning System [14]. Trilateration or multilateration algorithms have been proposed in the field of aerospace [15], [16]. The present paper briefly describes a multilateration algorithm based on simultaneous linear equations [2] that is applicable to a more general case, in which multiple ultrasonic receivers are placed in arbitrary positions. This is explained in detail below.

Here, l_1, l_2, $\cdots$, l_i denote the distances from the ultrasonic receiver at (x,y,z) to the ith ultrasonic transmitter at position (x_i,y_i,z_i). Using the spherical equations, we obtain simultaneous linear equations for the intersecting planes between the spheres as

$$\mathbf{AP} = \mathbf{B}, \tag{1}$$

$$\text{where} \quad \mathbf{P} = \begin{pmatrix} x \\ y \\ z \end{pmatrix}, \tag{2}$$

$$\mathbf{A} = \begin{pmatrix} 2(x_2-x_1) & 2(y_2-y_1) & 2(z_2-z_1) \\ 2(x_3-x_1) & 2(y_3-y_1) & 2(z_3-z_1) \\ \vdots & \vdots & \vdots \\ 2(x_i-x_1) & 2(y_i-y_1) & 2(z_i-z_1) \\ \vdots & \vdots & \vdots \end{pmatrix}, \tag{3}$$

$$\mathbf{B} = \begin{pmatrix} l_1^2-x_1^2-y_1^2-z_1^2-l_2^2+x_2^2+y_2^2+z_2^2 \\ l_1^2-x_1^2-y_1^2-z_1^2-l_3^2+x_3^2+y_3^2+z_3^2 \\ \vdots \\ l_1^2-x_1^2-y_1^2-z_1^2-l_i^2+x_i^2+y_i^2+z_i^2 \\ \vdots \end{pmatrix}. \tag{4}$$

For the case of four or more transmitters that are not coplanar, the rank of $\mathbf{A}$ becomes 3. The position (x,y,z) can be calculated by the least squares method as

$$\mathbf{P} = (\mathbf{A^T A})^{-1}\mathbf{A^T B}. \tag{5}$$

This method calculates position by solving plane equations derived from the equations of intersecting spheres. Reference [2] presents a detailed description for the case in which the rank of $\mathbf{A}$ is 2.

2) Calculating the positions of the calibration device in the global coordinate system (Step 4): The error function E can be defined as follows:

$$E = \sum_{i=0}^{n}\sum_{j=i+1}^{n} ||\mathbf{M}_i\mathbf{P}_i^{(i,j)} - \mathbf{M}_j\mathbf{P}_j^{(i,j)}||^2, \tag{6}$$

where $\mathbf{M_i}$ is the transformation matrix from the local coordination system i to the global coordination system, and $\mathbf{P}_j^{(i,j)}$ denotes points in the local coordination system j for the case in which the points can be calculated in both local coordination systems i and j.

$$\begin{aligned}
&\frac{\partial E}{\partial \mathbf{M_i}} \\
&= \frac{\partial}{\partial \mathbf{M_i}} \sum_{\substack{j=0 \\ (i\neq j)}}^{n} Tr\left\{\left(\mathbf{M}_i\mathbf{P}_i^{(i,j)} - \mathbf{M}_j\mathbf{P}_j^{(i,j)}\right)^T\left(\mathbf{M}_i\mathbf{P}_i^{(i,j)} - \mathbf{M}_j\mathbf{P}_j^{(i,j)}\right)\right\} \\
&= \frac{\partial}{\partial \mathbf{M_i}} \sum_{\substack{j=0 \\ (i\neq j)}}^{n} Tr\left\{-(\mathbf{M}_j\mathbf{P}_j^{(i,j)})^T\mathbf{M}_i\mathbf{P}_i^{(i,j)} - (\mathbf{M}_i\mathbf{P}_i^{(i,j)})^T\mathbf{M}_j\mathbf{P}_j^{(i,j)}\right. \\
&\quad \left. +(\mathbf{M}_i\mathbf{P}_i^{(i,j)})^T\mathbf{M}_i\mathbf{P}_i^{(i,j)} + (\mathbf{M}_j\mathbf{P}_j^{(i,j)})^T\mathbf{M}_j\mathbf{P}_j^{(i,j)}\right\} \\
&= -2\mathbf{M}_0\mathbf{P}_0^{(i,n)}(\mathbf{P}_i^{(i,n)})^T - \cdots - 2\mathbf{M}_{i-1}\mathbf{P}_{i-1}^{(i,i-1)}(\mathbf{P}_{i-1}^{(i,i-1)})^T \\
&\quad +2\mathbf{M}_i \sum_{\substack{j=0 \\ (i\neq j)}}^{n} \mathbf{P}_i^{(i,j)}(\mathbf{P}_i^{(i,j)})^T \\
&\quad -2\mathbf{M}_{i+1}\mathbf{P}_{i+1}^{(i,i+1)}(\mathbf{P}_i^{(i,i+1)})^T - \cdots - 2\mathbf{M}_n\mathbf{P}_n^{(i,n)}(\mathbf{P}_i^{(i,n)})^T.
\end{aligned} \tag{7}$$

If we select the local coordinate system 0 as the global coordinate system, M_0 becomes an identity matrix. From

Eq. (7), we can obtain simultaneous linear equations and calculate $\boldsymbol{M_i}$ using Eq. (8),

$$
\begin{pmatrix} \mathbf{M_1} & \mathbf{M_2} & \cdots & \mathbf{M}_n \end{pmatrix} = \begin{pmatrix} \mathbf{P}_0^{(0,1)}(\mathbf{P}_1^{(0,1)})^T & \mathbf{P}_0^{(0,2)}(\mathbf{P}_2^{(0,2)})^T & \cdots & \mathbf{P}_0^{(0,n)}(\mathbf{P}_n^{(0,n)})^T \end{pmatrix} \times
\begin{pmatrix}
\sum_{i=0}^{n} \mathbf{P}_1^{(1,i)}(\mathbf{P}_1^{(1,i)})^T & -\mathbf{P}_1^{(1,2)}(\mathbf{P}_2^{(1,2)})^T & \cdots & -\mathbf{P}_1^{(1,n)}(\mathbf{P}_n^{(1,n)})^T \\
-\mathbf{P}_2^{(1,2)}(\mathbf{P}_1^{(1,2)})^T & \sum_{i=0}^{n} \mathbf{P}_2^{(2,i)}(\mathbf{P}_2^{(2,i)})^T & \cdots & -\mathbf{P}_2^{(2,n)}(\mathbf{P}_n^{(2,n)})^T \\
\vdots & \vdots & \ddots & \vdots \\
-\mathbf{P}_n^{(1,n)}(\mathbf{P}_1^{(1,n)})^T & -\mathbf{P}_n^{(2,n)}(\mathbf{P}_2^{(2,n)})^T & \cdots & \sum_{i=0}^{n} \mathbf{P}_n^{(n,i)}(\mathbf{P}_n^{(n,i)})^T
\end{pmatrix}^{-1} . \tag{8}
$$

C. Considering the environment boundary condition

Regarding the GCLC method as presented above, the error of calibration will accumulate as the space in which the ultrasonic receivers are placed becomes larger. Therefore, the number of moving calibrating devices becomes larger. For example, if we place receivers on the ceiling of a corridor of size 2 x 30 m, the accumulated error may be large. This section describes the boundary constraint with which we can reduce the error accumulation.

In most cases, the ultrasonic location system will be placed in a building or on the components of a building, such as on a wall or ceiling. If we can obtain CAD data of the building or its components or if we can measure the size of a room inside the building to a high degree of accuracy, then we can use the size data as a boundary condition for calibrating the receiver positions.

Here, let us consider the boundary constraint shown in Fig. 2. We can formulate this problem using the Lagrange's undecided multiplier method as follows:

$$
E' = \sum_{i=0}^{3} \sum_{j=i+1}^{3} \left\| M_i P_i^{(i,j)} - M_j P_j^{(i,j)} \right\|^2 + \lambda F(M_3), \tag{9}
$$

$$
F(M_3) = (M_3 P_{b1} - P_{b0}) \cdot n + l_0 - l_1 = 0 \tag{10}
$$

where λ denotes a Lagrange's undecided multiplier. By solving this equation, we can obtain the following equations:

$$
\begin{pmatrix} \mathbf{M_1} & \mathbf{M_2} & \mathbf{M_3} \end{pmatrix} = \begin{pmatrix} \mathbf{P}_0^{(0,1)}(\mathbf{P}_1^{(0,1)})^T & 0 & -1/2\lambda \mathbf{n} \mathbf{P}_{b1}^T \end{pmatrix} \times
\begin{pmatrix}
\begin{matrix} \mathbf{P}_1^{(0,1)}(\mathbf{P}_1^{(0,1)})^T \\ +\mathbf{P}_1^{(1,2)}(\mathbf{P}_1^{(1,2)})^T \end{matrix} & -\mathbf{P}_1^{(1,2)}(\mathbf{P}_2^{(1,2)})^T & 0 \\
-\mathbf{P}_2^{(1,2)}(\mathbf{P}_1^{(2,1)})^T & \begin{matrix} \mathbf{P}_2^{(1,2)}(\mathbf{P}_2^{(1,2)})^T \\ +\mathbf{P}_2^{(2,3)}(\mathbf{P}_2^{(2,3)})^T \end{matrix} & -\mathbf{P}_2^{(2,3)}(\mathbf{P}_3^{(2,3)})^T \\
0 & -\mathbf{P}_3^{(2,3)}(\mathbf{P}_2^{(2,3)})^T & \mathbf{P}_3^{(2,3)}(\mathbf{P}_3^{(2,3)})^T
\end{pmatrix}^{-1} . \tag{11}
$$

By substituting $\boldsymbol{M_3}$ into Eq. (10), we can solve λ and eliminate it from Eq. (11).

The general case of the GCLC method with multiple boundary constraints is as follows:

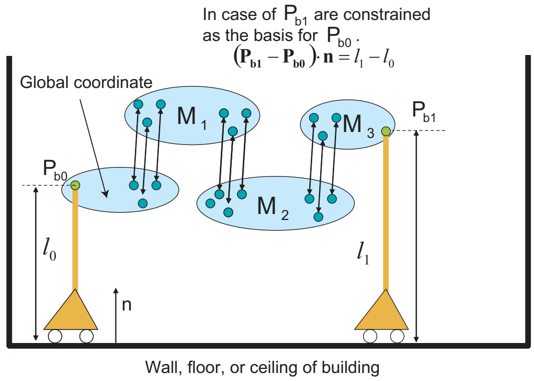

Fig. 2. Example of a boundary condition as the basis for the building

$$
\begin{pmatrix} \mathbf{M}_1 & \mathbf{M_2} & \cdots & \mathbf{M}_n \end{pmatrix} =
\begin{pmatrix}
\mathbf{P}_0^{(0,1)}(\mathbf{P}_1^{(0,1)})^T & \cdots & \cdots & \mathbf{P}_0^{(0,n)}(\mathbf{P}_n^{(0,n)})^T \\
-1/2 \sum_{i=0}^{n_i} \lambda_{1,i} \mathbf{n}_{1,i} \mathbf{P}_{1,i}^T & & & -1/2 \sum_{i=0}^{n_n} \lambda_{n,i} \mathbf{n}_{n,i} \mathbf{P}_{n,i}^T
\end{pmatrix} \times
\begin{pmatrix}
\sum_{\substack{i=0 \\ i \neq 1}}^{n} \mathbf{P}_1^{(1,i)}(\mathbf{P}_1^{(1,i)})^T & -\mathbf{P}_1^{(1,2)}(\mathbf{P}_2^{(1,2)})^T & \cdots & -\mathbf{P}_1^{(1,n)}(\mathbf{P}_n^{(1,n)})^T \\
-\mathbf{P}_2^{(1,2)}(\mathbf{P}_1^{(1,2)})^T & \sum_{\substack{i=0 \\ i \neq 2}}^{n} \mathbf{P}_2^{(2,i)}(\mathbf{P}_2^{(2,i)})^T & \cdots & -\mathbf{P}_2^{(2,n)}(\mathbf{P}_n^{(2,n)})^T \\
\vdots & \vdots & \ddots & \vdots \\
-\mathbf{P}_n^{(1,n)}(\mathbf{P}_1^{(1,n)})^T & -\mathbf{P}_n^{(2,n)}(\mathbf{P}_2^{(2,n)})^T & \cdots & \sum_{\substack{i=0 \\ i \neq n}}^{n} \mathbf{P}_n^{(n,i)}(\mathbf{P}_n^{(n,i)})^T
\end{pmatrix}^{-1} , \tag{12}
$$

where $\lambda_{i,j}$, $\mathbf{n_{i,j}}$, and $\mathbf{P_{i,j}}$ denote the j-th undecided multiplier, the j-th constraint vector, and the j-th constrained point in the i-th local coordinate system, respectively. In this case, the boundary constraints are as follows:

$$
F_{i,j} = (\mathbf{M_i} \mathbf{P_{i,j}} - \mathbf{P_{b0}}) \cdot \mathbf{n_{i,j}} - \Delta l_{i,j} = 0, \tag{13}
$$

where $\Delta l_{i,j}$ denotes a distance constraint. The above GCLC method with boundary constraints is applicable to, for example, the case in which more complex boundary conditions exist, as shown in Fig. 3.

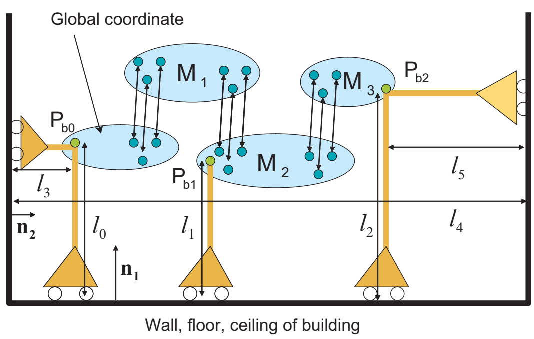

Fig. 3. Example of a greater number of boundary conditions as the basis of the building

D. Consideration of ultrasonic damping

1) Error due to ultrasonic damping: The authors discovered a phenomenon whereby the measured distance between receivers and transmitters appears longer than the actual distance due to ultrasonic damping. This phenomenon causes an increase in the error. The damping is caused by the directivities of the transmitter and the receiver. This section describes a method that considers the directivities in order to reduce this effect.

The newly developed ultrasonic location system measures the distance from the time-of-flight of the ultrasonic pulse. The time at which the ultrasonic wave exceeds the threshold is the arrival time of the ultrasonic pulse at the receiver, as shown in Fig. 4. However, in the case of damping of the ultrasonic wave, due to the effects of directivity and distance, the error of the measured distance increases as a result of the delay in the ultrasonic pulse arrival time expressed by ΔT.

2) Approach to the damping problem: There are two approaches to this problem: a hardware approach and a software approach. In the hardware approach, the highest point of the ultrasonic wave, for example, can be assumed to be the ultrasonic pulse arrival time, as determined by sampling and analyzing the ultrasonic wave, which requires expensive equipment. Therefore, in the present paper, we consider the software approach.

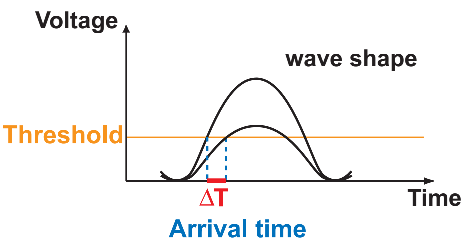

Fig. 4. Measurement of ultrasonic pulse arrival time

3) Method for dealing with the damping problem: The distance between the receivers and transmitters is

$$|\mathbf{Pr}_i - \mathbf{Pt}_j| = L_{ij}, \tag{14}$$

where $\mathbf{Pr}_i$ are the positions of the receivers, $\mathbf{Pt}_j$ are the positions of the transmitters, and L_{ij} are the actual distances. The ultrasonically measured distances $L_{m,ij}$ are longer than the actual distances L_{ij}. The actual distances L_{ij} are described by

$$L_{ij} = L_{m,ij} - \Delta L_{ij}, \tag{15}$$

where ΔL_{ij} is the error of the distance.

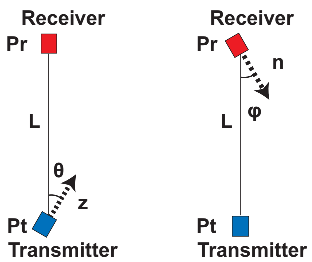

Fig. 5. Angle and distance

The experimentally obtained relationship between the transmitting angle of a transmitter and the error and that between the receiving angle of a receiver and the error are shown in Figure 6.

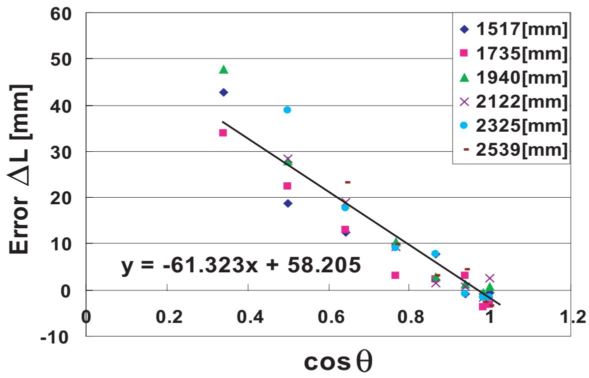

Fig. 6. Relationship between transmitting angle and error

Here,

$$\Delta L_{ij} = -61.323 \cos\theta_{ij} - 75.622 \cos\phi_{ij} + 131.662 \tag{16}$$

was obtained experimentally.

IV. Experiments

A. System configuration

Figure 7 shows the system configuration for the proposed 3D ultrasonic tag system. The system consists of an ultrasonic receiving section, an ultrasonic transmitting section, a time-of-flight measurement section, a network section, and a personal computer. The ultrasonic receiving section receives ultrasonic pulses emitted from the ultrasonic transmitter and amplifies the received signal. The time-of-flight measurement section records the travel time of the signal from transmission to reception. The network section synchronizes the system and collects time-of-flight data from the ultrasonic receiving section. The positions of objects are calculated based on more than three time-of-flight measurements.

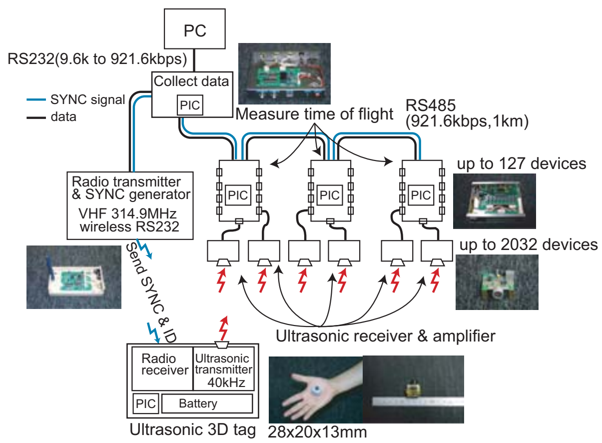

Fig. 7. System configuration

B. Experimental results

1) Method for error evaluation: Errors are defined as the distances between the calculated receiver positions and the true receiver positions and are denoted by e_1, e_2, $\cdots$,

e_n. The average error is defined by

$$E = \frac{1}{n}\sum_{i=1}^{n} e_i. \tag{17}$$

2) Accuracy evaluation: Calibration was performed in a room (4.0×4.0×2.5 m) having 80 ultrasonic receivers embedded in the ceiling. Figure 8 shows the experimental results obtained using the GCLC method without any constraints. The authors performed calibration at 16 points in the room. Seventy-six receivers were calculated. In the figure, the red spheres indicate calculated receiver positions, the black crosses indicate the true receiver positions, and the blue spheres indicate the positions of the calibration device. Figure 9 shows the experimental results for the GCLC method considering directivities. Seventy-six receivers were calculated. Table I shows the average error E, maximum error, and minimum error for these methods. The above results show that using the GCLC method we can calibrate the position of receivers placed in a space of average room size and that the error can be reduced significantly by considering directivity.

Another calibration was performed in a rectangular space (1.0×4.5) having a longitudinal length that is much longer than its lateral length. Seventy-six ultrasonic receivers were embedded in the space. Figure 10 shows the experimental results obtained using the GCLC method without any constraints. Seventy-five receivers were calculated. Figure 11 shows the experimental results obtained using the GCLC method directivity consideration and a boundary constraint. Table II shows the average error E, maximum error, and minimum error for these methods. The above results show that with the GCLC method with directivity consideration and boundary constraint has a significantly reduced error.

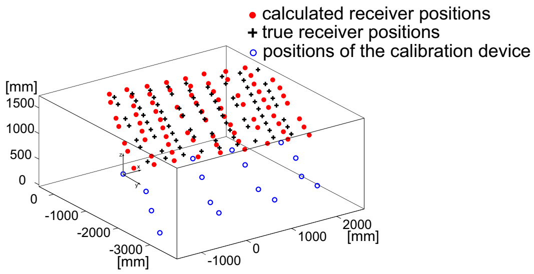

Fig. 8. Experimental result obtained by the GCLC method

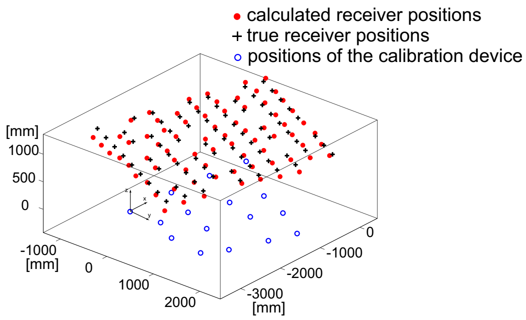

Fig. 9. Experimental result obtained by the GCLC method considering directivity

TABLE I

ERRORS (MM) OF THE PROPOSED METHOD FOR THE CASE OF A SQUARE-LIKE SPACE

	Ave. error	Max. error	Min. error
GCLC	195 mm	399 mm	66 mm
GCLC with directivity consideration	75 mm	276 mm	9 mm

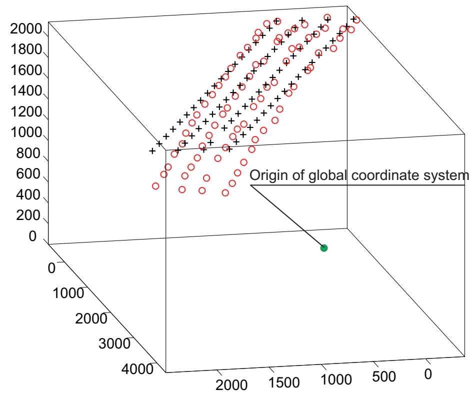

Fig. 10. Experimental results obtained by the GCLC method

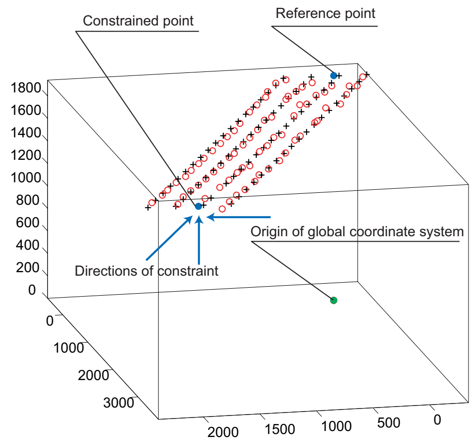

Fig. 11. Experimental results obtained by the GCLC method with directivity consideration and a boundary constraint

TABLE II

ERRORS (MM) OF THE PROPOSED METHOD FOR THE CASE OF A RECTANGULAR SPACE HAVING A LONGITUDINAL LENGTH THAT IS MUCH LONGER THAN ITS LATERAL LENGTH

	Ave. error	Max. error	Min. error
GCLC	236 mm	689 mm	17 mm
GCLC with directivity consideration and boundary constraint	51 mm	121 mm	10 mm

V. Advantages of the GCLC Method

The advantages of the GCLC method are listed below.

- The method requires a relatively small number of transmitters, at least three transmitters, so that the user can calibrate the ultrasonic location system using a small calibrating device having at least three transmitters.
- The method can calibrate the positions of the receivers independent of room size.
- The error can be reduced by considering the directivity constraint. The constraint is useful for cases in which the ultrasonic location system adopts a method in which the time-of-fight is detected by thresholding the ultrasonic pulse.
- The error can be reduced by considering the boundary constraint. The constraint is useful for cases in which the receivers to be calibrated are placed in a rectangular space having a longitudinal length that is much greater than the lateral length, such as a long corridor.

VI. Realized Ultrasonic Portable 3D Tag System

The GCLC method enables a portable ultrasonic 3D tag system. Figure 12 shows a portable ultrasonic 3D tag system, which consists of a case, tags, receivers, and a calibration device. The portable system enables measurement of human activities by quickly installing and calibrating the system on-site, at the location where the activities actually occur.

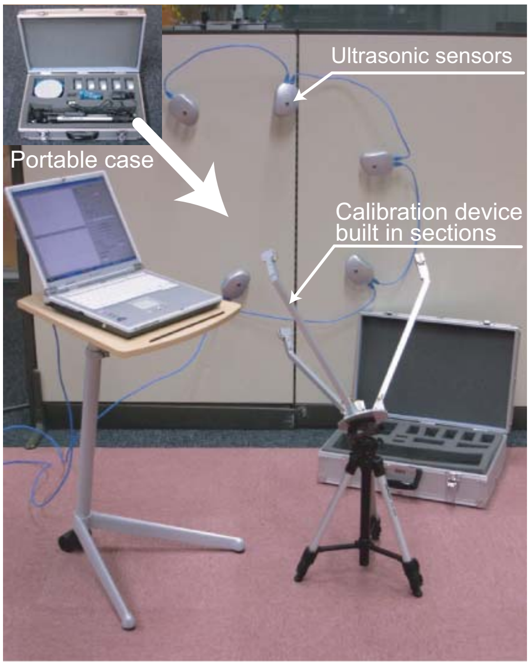

Fig. 12. Developed portable ultrasonic 3D tag system

VII. Conclusion

In the present paper, we proposed a new calibration method, "global calibration based on local calibration (GCLC)", for an ultrasonic location system so that users can quickly calibrate a system and observe human activity in various environments where the activities actually occur. One of the advantages of the GCLC method is the requirement for a relatively small number of transmitters. In addition, the GCLC method is not dependent on room size. We also described two constraints that can be used in conjunction with the GCLC method: the directivity constraint and the boundary constraint.

In addition, a portable ultrasonic location sensor based on the proposed method was realized. The portable system allows human activities to be measured in the area where the activities actually occur with quick installation and calibration.

Further studies will examine the refinement of the method in order to measure the 3D positions with higher accuracy, systematization of calibration methods, and the use of the portable 3D ultrasonic tag system in a living space.

References

[1] H. Mizoguchi, T. Sato, T. Ishikawa, "Robotic Office Room to Support Office Work by Human Behavior Understanding Function with Networked Machines," *IEEE/ASME Transactions on Mechatronics*, Vol. 1, No. 3, September 1996, pp. 237-244.

[2] Y. Nishida, H. Aizawa, T. Hori, N.H. Hoffman, T. Kanade, M. Kakikura, "3D Ultrasonic Tagging System for Observing Human Activity," in *Proceedings of IEEE International Conference on Intelligent Robots and Systems* (*IROS2003*), pp. 785-791, October 2003.

[3] Y. Nishida, K. Kitamura, T. Hori, A. Nishitani, T. Kanade, H. Mizoguchi, "Quick Realization of Function for Detecting Human Activity Events by Ultrasonic 3D Tag and Stereo Vision," in *Proceedings of 2nd IEEE International Conference on Pervasive Computing and Communications* (*PerCom2004*), pp. 43-54, March 2004.

[4] A. Ward, A. Jones, A. Hopper, "A New Location Technique for the Active Office," *IEEE Personal Communications*, Vol. 4, No. 5, pp. 42-47, October 1997.

[5] A. Harter, A. Hopper, P. Steggles, A. Ward, P. Webster, "The Anatomy of a Context-Aware Application," in *Proceedings of the ACM/IEEE MobiCom*, August 1999.

[6] M. Addlesee, R. Curwen, S. Hodges, J. Newman, P. Steggles, A. Ward, A. Hopper, "Implementing a sentient computing system," *IEEE Computer*, Vol. 34, No. 8, pp. 50-56, August 2001.

[7] M. Hazas and A. Ward, "A Novel Broadband Ultrasonic Location System," in *Proceedings of UbiComp 2002*, pp. 264-280, September 2002.

[8] N.B. Priyantha, A. Chakraborty, H. Balakrishnan, "The Cricket Location-Support system," in *Proceedings of the 6th International Conference on Mobile Computing and Networking* (*ACM MobiCom2000*), pp. 32-43, August 2000.

[9] A. Mahajan and F. Figueroa, "An Automatic Self Installation and Calibration Method for a 3D Position Sensing System using Ultrasonics," *Robotics and Autonomous Systems*, Vol. 28, No. 4, pp. 281-294, September 1999.

[10] Y. Fukuju, M. Minami, H. Morikawa, and T. Aoyama, "DOLPHIN: An Autonomous Indoor Positioning System in Ubiquitous Computing Environment," in *Proceedings of IEEE Workshop on Software Technologies for Future Embedded Systems* (*WSTFES2003*), pp. 53-56, May 2003.

[11] P. Duff, H. Muller, "Autocalibration Algorithm for Ultrasonic Location Systems," in *Proceedings of 7th IEEE International Symposium on Wearable Computer*, pp. 62-68, October 2003.

[12] Y. Chen, G. Medioni, "Object Modeling by registration of multiple range images," *Image and Vision Computing,* Vol. 10, No. 3, pp. 145-155, April 1992.

[13] P.J. Neugebauer, "Geometrical Cloning of 3D Objects via Simultaneous Registration of Multiple Range Images," in *Proceedings of the 1997 International Conference on Shape Modeling and Application* (*SMA'97*), pp. 130-139, 1997.

[14] B.W. Parkinson, J.J. Spilker, P. Axelrad, P. Enge, *The Global Positioning System: Theory and Applications,* American Institute of Aeronautics and Astronautics, 1996.

[15] K.C. Ho "Solution and Performance Analysis of Geolocation by TDOA, " *IEEE Transaction on Aerospace and Electronic Systems*, Vol. 29, No. 4, October 1993, pp. 1311-1322.

[16] D.E. Manolakis, "Efficient Solution and Performance Analysis of 3-D Position Estimation by Trilateration, " *IEEE Trans. on Aerospace and Electronic Systems*, Vol. 32, No. 4, October 1996, pp. 1239-1248.